

Effect of Torso Mesh Density on Electrocardiographic Imaging Resolution from Atrial Fibrillation Simulations

Rubén Molero¹, Ana González-Ascaso¹, Ismael Hernández-Romero¹, Andreu M Climent¹,
María S Guillem¹

¹ ITACA Institute, Universitat Politècnica de València, València, Spain

Abstract

Electrocardiographic Imaging (ECGI) allows estimating the epicardial electrical activity using anatomical information and body surface electrograms. In this study, the effect of the number and distribution of nodes constituting torso meshes on the ECGI accuracy is analyzed using atrial fibrillation (AF) simulations.

3D meshes of the torso of 10 patients with 100 to 2000 nodes with either a heterogeneous or a homogeneous distribution were created. Signals of 9 AF realistic electrophysiological simulations were used for computing the forward and inverse problems. The resulting ECGI for each torso mesh was compared with the ECGI computed with a 4000 nodes reference torso. Correlation coefficient of electrograms, and relative difference of dominant frequency were computed to evaluate each torso mesh and electrode distribution with the respective ground truth.

Torso meshes with higher number of nodes and a homogeneous node distribution achieved better ECGI reconstructions in terms of correlation coefficients (values ranging from 0.56 ± 0.06 to 0.92 ± 0.04). Relative errors in dominant frequency estimations showed the same trend. Meshes of more than 400 nodes don't improve significantly the ECGI reconstruction. Distances between nodes of the torso meshes longer than 4 cm should be avoided.

1. Introduction

Electrocardiographic imaging (ECGI) is a non-invasive technique that can be used to estimate the electrical activity of the heart from surface electrocardiographic signals. ECGI offers multiple clinical applications, such as ablation guidance in Atrial Fibrillation (AF) patients. ECGI requires to use torso and heart geometries together with electrical recordings from the patient. On the one hand, surface electrodes placed over the torso are used to record electrical signals. On the other hand, the heart geometry is usually obtained from medical images [1], and the torso geometry can be derived from video recordings, with the latter reconstruction creating triangular or polygonal meshes [2]. Once these elements are acquired, the inverse

problem can be solved, and epicardial potentials are estimated, which can be used to compute dominant frequencies or rotor-related metrics [3].

The properties of the 3D torso geometry have been proven to affect the calculation of the ECGI. Accurate reconstructions [4] of the anatomy of the patient's body and the consideration of real dimensions in the model show more precise results. The incorporation of inner organs into the geometry of the problem has not shown a major impact on the shape of ECGI potentials[5]. However, additional geometrical effects should be carefully considered to achieve a sufficient resolution of ECGI signals.

The objective of this study is to evaluate the repercussion of the number of nodes of the torso geometry mesh and their distribution on the resolution of the ECGI using AF simulations. We hypothesized that there is an effect on the ECGI reconstruction quality related to the number of nodes on the torso mesh used independently of the number of ECG electrodes that record the signal. We compared the electrocardiographic signals (ECGI) using time metrics: the Pearson's correlation coefficient (CC) and the relative difference measurement star (RDMS) and errors in dominant frequency estimation.

2. Material and methods

To analyze the effect related to node variations of torso geometry on the ECGI, we first created the torso models with different numbers and distribution of the nodes, then computed the respective inverse computed electrograms and finally compared the result using time metrics (CC and RDMS) and dominant frequencies related maps and metrics.

2.1. Atrial fibrillation simulations

Cardiac electrophysiological simulations lasting for 10 seconds were included in this study were created using the same cardiac geometry and different AF episodes. A realistic 3D model of the atrial anatomy composed by 284.578 nodes and 1.353.783 tetrahedrons was used for creating the simulations [6]. Variation of currents was introduced in Ik, ACH, IK1, INa, and IcaL to simulate

electrical remodeling and allow the maintenance of fibrillation. Fibrotic tissue was modeled by disconnecting a percentage of nodes between 20% and 60%, and scar tissue by disconnecting 100% of nodes in the scar region. The system of differential equations was solved by using Runge–Kutta integration based on a graphic processors unit (NVIDIA Tesla C2075 6G), [6]. AF was induced by implementing an S1 S2 protocol, with the S2 stimulus applied at different locations in the atria, thus producing different AF patterns.

2.2. Data processing

To create different torso models for computing surface ECG signals, we used the torso geometries from 10 patient anatomies. Then, the epicardial potentials computed for each of the electrophysiological models were placed in the same position as the original heart inside the thorax. For each torso, 14 different mesh distributions were created: torsos with 100, 200, 400, 500, 1000, and 2000 nodes heterogeneously and homogeneously distributed (Fig. 1) and one model with 4000 nodes that is used as the gold standard.

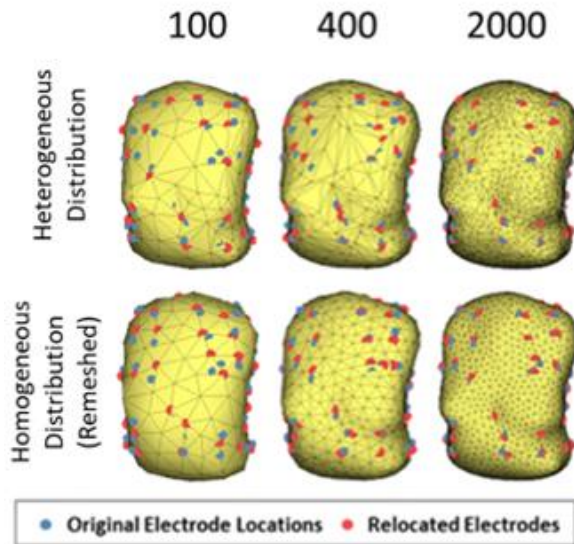


Fig. 1. Example of torso models with different number of nodes and node distribution. The electrodes relocated appear in blue, and the original locations are in red.

ECG signals were chosen on 57 electrodes in the selected torsos. When remeshing, the nodes corresponding to the electrodes were selected as the closest node to the original electrode position computing the Euclidean distance. The forward problem of the simulated electrograms was calculated using the boundary element method (BEM) [7]. Noise was added to the computed surface potentials to

obtain a 20dB signal-to-noise ratio emulating real recordings. Base line was subtracted, and a low pass filter of 40 Hz was applied. The electrical information related to the nodes representing the 57 electrodes was selected, and the inverse problem was calculated through the BEM, using zero-order Tikhonov regularization and L-curve optimization [7].

2.3. ECGI evaluation metrics

To evaluate the effect of the mesh in the reconstruction of ECGI, the similarity between ECGI signals obtained with 4000 nodes were compared with torso meshes of 100, 200, 400, 500, 1000, and 2000 nodes. We used Pearson’s correlation coefficient (CC) and the relative difference measurement star (RDMS) [8] for the ECGI comparison. For both time metrics, the temporal version was used (for each node, the CC and RDMS were computed using all the time instants, and the mean and standard deviation across nodes were then calculated). The dominant frequencies of each node of the cardiac geometry were estimated after the calculation of ECGI using Welch periodogram (2-second Hamming window with a 25% overlap) [9]. The absolute difference in frequencies for each atrial node between the reference and the other models was calculated [8].

3. Results

The variations between ECGI signals obtained from cardiac electrophysiological simulations and using different torso meshes are shown in Figure 2. The reference signals are ECGI reconstructions using the most refined torso mesh (4000R). The Pearson’s correlation coefficient (CC) and the relative difference measurement star (RDMS) take different values depending on the properties of each torso geometry, see Fig. 2 panels A and B, respectively. On the one hand, a progressive increase is shown for the CC as the number of nodes increases, from $0,56 \pm 0,06$ for the 100 mesh to $0,92 \pm 0,04$ for the 2000 mesh. On the other hand, the RDMS decreases when the torso is composed of a higher number of vertices, from $0,96 \pm 0,07$ for the 100 mesh down to $0,38 \pm 0,09$ for the 2000 mesh. Regular meshes do show better correlation coefficients and RDMS values than irregular meshes with a similar number of nodes, especially for the meshes with lower number of nodes. For the finer meshes and, therefore, smaller areas of the geometrical faces, slightly better results are observed for the irregular meshes, most likely because they are constituted by a larger number of nodes.

3.1. Frequency metrics

To further investigate the effect of the torso geometry on the resolution of ECGI, the dominant frequencies for each cardiac node were calculated. Figure 3 shows the

differences in Hz between the ECGI calculated with the torso with 4000 nodes homogeneously distributed and the

remaining models. The highest difference can be observed for the torso with 100 nodes ($1.14 \pm 0,26$ Hz), and it decreases as the number of nodes increases. Differences in the frequencies show higher values when a homogeneous distribution of the electrodes is presented for models of less than 1000 nodes. However, when the number of nodes was 1000 or higher, these differences are higher in the case of the homogeneous models, which again can be attributed to the largest number of nodes in the irregular meshes' geometries.

In Fig. 4, dominant frequency maps of an AF simulation computed with the different torso geometries studied are presented. It can be observed that, from 400 nodes, the DF maps tend to shrink the highest DF area being more like the reference map computed with the 4000R nodes torso mesh.

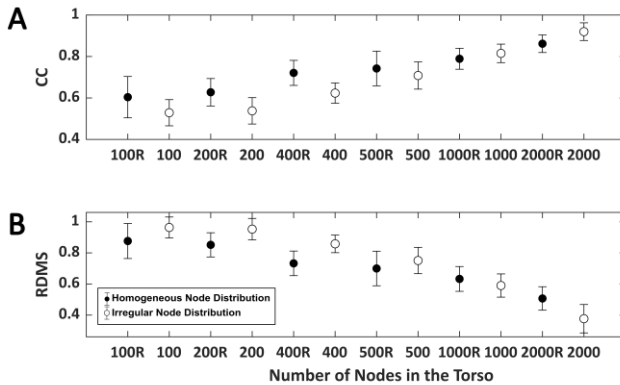


Fig. 2. Time metrics obtained comparing the inverse computed electrograms of the reference and the signals obtained with different torso models. Points in black represent the torsos in which the distribution of the nodes is homogeneous and white points represent the torso with nodes heterogeneously placed. A. Pearson's correlation coefficient (CC) and B. Relative difference measurement

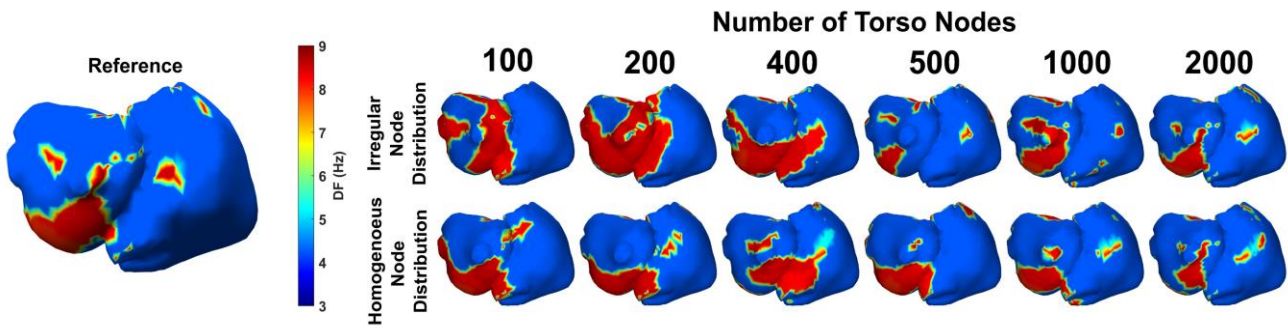


Fig. 4. Dominant frequency maps obtained with different torso models for an atrial fibrillation simulation.

star (RDMS).

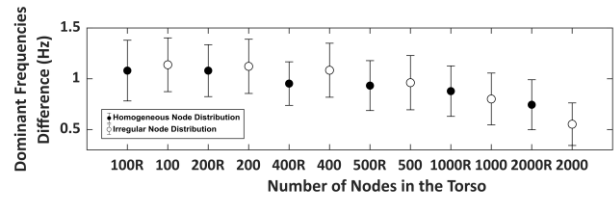


Fig. 3. Mean absolute difference between the reference dominant frequencies the frequencies calculated with the other torso models. Points in black represent the torsos in which the distribution of the nodes is homogeneous and white points represent the torso with nodes heterogeneously placed.

4. Discussion

In this study, we show that there exists a relationship between the number and distribution of nodes of the torso geometry mesh used in the calculation of the ECGI and the obtained ECGI values. Better results are achieved with torsos with a higher number of nodes in the mesh independently of the number of recorded electrodes. The correlation coefficient increases together with the number of nodes. It is observed that the CC tendency from 400-nodes torsos and superior, the CC tends to stabilize. The same results are shown for RDMS and DF differences. This suggests that with torsos of more than 400 nodes, the obtained inverse solution does not improve significantly.

With the observed results, the mean displacement of the electrodes should be smaller than 20 mm (torso with more than 400 nodes) to achieve reliable results in the resolution of the inverse problem.

The effect of the node density of the meshes of the torsos has not been widely studied. Nevertheless, an accurate torso geometry has been reported as necessary to obtain precise inverse electrograms [4]. Torso reshaping and remeshing with a different number of nodes affected the quality of the signals, being 400 nodes the minimum

necessary to obtain a good result. Torso reshaping and

smoothing the geometry have been reported to produce less accurate results when computed inverse electrograms [10]. Nevertheless, we demonstrated that a homogeneous distribution of the nodes improved the inverse solution, at least for low-resolution meshes.

The position and displacement of the electrodes remain important [2]. The remeshing in our study influenced electrode location, but we could establish the maximum displacement tolerated of the electrodes as 2cm. This distance gives margin to consider as a good reconstruction of the location of the electrodes using photogrammetry. Furthermore, slightly displaced electrodes would not affect the results drastically. Despite that, we can ensure that 400 nodes -or mean distance between nodes below 4 cm- is a good trade-off for torso geometry reconstruction.

4.1. Limitations

In this study, we compared simulated AF signals with ECGI reconstructed with a higher number of nodes in the mesh as a gold standard and with no intracardiac data. We considered a higher number of nodes models as a reference assuming that it will provide a better reconstruction. Furthermore, we could not differentiate what affects more, the number of nodes or the location of the electrodes, because torso remeshing displaced their location. Future studies should explore the effect of number of nodes in the torso without displacement, together with an analysis with real AF recordings.

5. Conclusion

The present study shows that a mesh of at least 400 nodes is recommended for computing the inverse problem with atrial fibrillation signals to obtain reliable results. Furthermore, a homogeneous distribution of the nodes showed to be convenient for computing the ECGI with a distance separation of nodes under 4 cm. A displacement of the nodes corresponding to the position of the electrodes higher than 2 cm should be avoided.

Acknowledgments

This work was supported by: Instituto de Salud Carlos III, and Ministerio de Ciencia e Innovación (supported by FEDER Fondo Europeo de Desarrollo Regional PI17/01106, PEJ2018-003617 and RYC2018-024346-I), EIT Health (Activity code 220385, EIT Health is supported by EIT, a body of the European Union), Generalitat Valenciana Conselleria d'Educació, Investigació, Cultura i

Esport (ACIF/ 2020/265) and Spanish Agencia Estatal de Investigación (AEI), part of the Ministerio de Ciencia e Innovación, reference PID2020-119364RB-I00.

References

- [1] J. Salinet et al., "Electrocardiographic imaging for atrial fibrillation: A perspective from computer models and animal experiments to clinical value." *Front Physiol* vol. 12, pp. 1-23, Apr. 2021.
- [2] A. W. M. van der Graaf et al., "A priori model independent inverse potential mapping: the impact of electrode positioning," *Clin. Res. Cardiol.*, vol. 105, no. 1, pp. 79-88, Jul. 2016.
- [3] R. Molero et al., "Prediction of ablation success in atrial fibrillation patients based on electrocardiographic imaging," *EP Eur.*, vol. 24, no. Supplement_1, May 2022.
- [4] B. J. Messinger-Rapport and Y. Rudy, "Noninvasive recovery of epicardial potentials in a realistic heart-torso geometry. Normal sinus rhythm," *Circ. Res.*, vol. 66, no. 4, pp. 1023-1039, Apr. 1990.
- [5] C. Ramanathan and Y. Rudy, "Electrocardiographic imaging: I. Effect of torso inhomogeneities on body surface electrocardiographic potentials," *J. Cardiovasc. Electrophysiol.*, vol. 12, no. 2, pp. 229-240, Feb. 2001.
- [6] M. Rodrigo et al., "Technical considerations on phase mapping for identification of atrial reentrant activity in direct-And inverse-computed electrograms," *Circ. Arrhythmia Electrophysiol.*, vol. 10, no. 9, p. e005008, Sept. 2017.
- [7] J. Pedrón-Torrecilla et al., "Noninvasive estimation of epicardial dominant high-frequency regions during atrial fibrillation," *J. Cardiovasc. Electrophysiol.*, vol. 27, no. 4, pp. 435-442, Apr. 2016.
- [8] C. Figuera et al., "Regularization techniques for ECG imaging during atrial fibrillation: A computational study," *Front. Physiol.*, vol. 7, no. Oct. 2016.
- [9] M. Rodrigo et al., "Highest dominant frequency and rotor positions are robust markers of driver location during noninvasive mapping of atrial fibrillation: A computational study," *Hear. Rhythm*, vol. 14, no. 8, pp. 1224-1233, Aug. 2017.
- [10] J. Lenkova, J. Svehlikova, and M. Tysler, "Individualized model of torso surface for the inverse problem of electrocardiology," *J. Electrocardiol.*, vol. 45, no. 3, pp. 231-236, May 2012.

Address for correspondence:

Rubén Molero Alabau
ITACA. Edificio 8G acceso B. Universitat Politècnica de València. Camino de Vera s/n. 46022 Valencia, Spain.
rmoal1@itaca.upv.es